International Journal of Innovative Technology and Exploring Engineering (IJITEE)
ISSN: 2278-3075 (Online), Volume-9 Issue-3, January 2020

Smart Vibration Sensor for Axleboxes

Sergey Lebedev, Sergey Sinutin, Evgeniy Sinutin, Petr Koropets

Abstract*: This article describes the actual problem for railway transport, maximum thrust without boxing. The classification for dynamic modes operation of the locomotive drive is presented. An example of a system built for locomotive is presented. It is possible to use an encoder and vibration sensor inside a smart axle-box. These sensors based on a specially domestic designed ASIC. It is shown that vibration sensors could be positioned on the cover of an axle-box. Considering this fact, one could develop a system for predicting "before boxing" state of a wheel pair. That system could be based on domestically produced electronic components. This article is about developing a smart device for railway transport, in particular, for traction vehicle. The operating principle is based on express analysis of dynamic processes in the contact of the wheel with the rail, the characteristics of which are determined by the angular accelerations of the wheel pair and forward accelerations of the axle box, i.e. the bearing housing, which is rotating in the wheelset axle.

***Keywords*: Antiboxing System, Encoder, Skid Exclusion, Stable Grip, Traction Force, Vibration Sensor.**

I. INTRODUCTION

Improving the consumer qualities and properties of devices in our information age has led to the introduction of the concept of a smart device.

A device is considered smart if it is capable of independently selecting one of the possible operating modes without operator's participation on the basis of information received and processed by it, and also if the device is able to diagnose itself and control metrological accuracy. At the same time, it is legitimate to refer smart devices to devices whose traditional capabilities are expanded with additional functions that allow to get a fundamentally new quality.

One of the important issues of traction vehicle is the possibility of an uncontrolled transition of the normal operation mode of the wheelset to the wheelspin mode (intensive wheel rotation with their sliding relative to the rails).

Revised Manuscript Received on January 30, 2020.
***** Correspondence Author
Sergey Lebedev*, Design Center "Design of Integrate Microelectronic System", National Research University of Electronic Technology (MIET), Moscow, Russian Federation. Email: lebedevsergey11@rambler.ru
Sergey Sinutin, Institute of Radio Engineering Systems and Control, Southern Federal University. Email: sasinyutin@sfedu.ru
Evgeniy Sinutin, Scientific and Technical Center "Technocentre" of Southern Federal University. Email: dark_elf4@mail.ru
Petr Koropets, Department of Traction Rolling Stock, Electromechanical faculty, Rostov State Transport University, Rostov-on-Don, Russia. Email: pkoropets@gmail.com

The maximum traction force of the locomotive is limited by the capacity on the adhesion of wheels to rails and the risk of spinning. Spinning occurs when the torque of the wheelset starts to exceed the moment of adhesion of the wheels to the rails.

The spinning process has been known since the time of the first railways. The negative aspects of this phenomenon are also well known: a decrease in effective traction, high dynamic loads in the transmission, as well as intensive wear of wheels and rails. Therefore, the sustainable development (without disruption to spinning) of the maximum possible traction force remains an urgent task, the solution of which allows to save energy (fuel) and reduce the cost of repairing vehicle and track [1].

The majority of currently used anti-slip systems apply the principle of comparing wheel pair rotation speeds with each other: if the angular speed of any wheel pair sharply increases, then this wheel pair has slipped, and measures must be taken to stop spinning, i.e. put sand under the wheels or reduce traction. Thus, almost all existing systems respond to spinning that has already begun, i.e. – bond failure, which increases the rotation speed of the wheelset.

The effectiveness of dealing with spinning depends on how quickly it is detected and time addressed to eliminate it.

There is a reasonable question, is it possible to detect a dangerous mode in terms of bond failure in order to take timely measures and prevent slippage in the maximum traction mode in advance before the bond failure?

In 2001, there was a device developed in Russia [2], which makes it possible to detect such a state of the "wheel-track" system, in which the probability of skidding reaches its minimum index, but the intensive sliding of the wheels has not yet begun, and there is time to take measures to prevent spinning. In 2009, the basic ideas embedded in the device were experimentally tested and confirmed [3].

II. METHODOLOGY

Author (s) can send paper in the given email address of the journal. There are two email address. It is compulsory to send paper in both email address.

Let's have a look at a pair of wheels under the influence of traction torque, bite moment and vertical dynamic load.

Its motion is described by a differential equation

$$J_к \ddot{\phi}_к = M_m - M_c, \quad (1)$$

$\phi_к$ and $J_к$ - respectively is the angular coordinate and wheelset starting resistance;

$M_т$ and M_c - traction moment and bite moment of the wheelset with rails.

Rising and falling traction characteristics $M_c\left(\dot{\phi}_{ск}\right)$ are schematically represented as straight line segments.

Traction moment $M_m = M_*$ is considered as constant and independent of the wheelset rotation speed $\dot{\phi}_к$, i.e. its characteristic is a horizontal line. See Fig. 1.

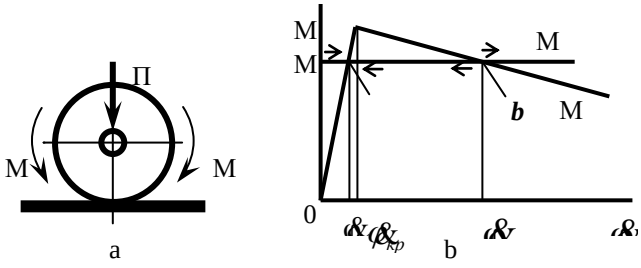

Fig. 1. The dynamic wheelset model

This simplification is made due to the following reasons: it is necessary to find an informative sign of the transition of the system from a stable dynamic state to an unstable one, not depending on what kind of traction characteristic it has and at what exact value of the traction moment or sliding speed this transition occurs (from traction to spinning).

Performing the procedure for (1) of transition to dynamic coordinates described in [4], we get the following:

$$J_к\ddot{\phi}_к = -\alpha\dot{\phi}_к - \frac{\Delta П}{П_o}M_*, \qquad (2)$$

where α – the sharpness of the ascending section of the dependence of the bite moment on the angular velocity of relative slip;

$П_o$ and $\Delta П$ - respectively, static and dynamic vertical load in contact of the wheelset with the rails (for one axis).

Let us set $\lambda = \frac{\Delta П}{П_o}$. Assuming that $\Delta П$ changes according to the harmonic law, we get

$$\lambda = \lambda_a \sin\left(\omega t\right), \qquad (3)$$

Solving (2) by the method of complex amplitudes, we find the expression for the amplitude of the forced oscillations of the angular velocity of the wheelset:

$$\dot{\phi}_{ка} = \frac{\lambda_a M_*}{\sqrt{J_к^2\omega^2 + \alpha^2}}, \qquad (4)$$

The expression (4) is obtained for the constant sharpness of the ascending section of the adhesion characteristic.

But α can make sense of equivalent damping $\alpha_э$ nonlinear system, if its movement is close to harmonic, and the amplitude of the oscillations is equal to the amplitude of the oscillations of the linear (linearized) system.

Such a comparison of linear and nonlinear systems in the theory of oscillations is called the harmonic linearization method. This method is traditionally used to determine the amplitude of oscillations of a nonlinear system. In this case, the harmonic linearization method is used to identify the parameter (damping) of linear and nonlinear systems.

Expression (4) that defines $\dot{\phi}_{ка}$ through α and other parameters are used to determine equivalent damping $\alpha_э$ through $\dot{\phi}_{ка}$ and the same model parameters obtained by numerical modeling of a nonlinear system, i.e. systems of a similar structure but with a nonlinear friction characteristic:

$$\alpha_э = \sqrt{\left(\frac{\lambda_a M_*}{\dot{\phi}_{ка}}\right)^2 - J_к^2\omega^2}, \qquad (5)$$

The considered nonlinear system (1) with increasing M_* (shifting it to the maximum moment of adhesion) the instantaneous values of the angular velocity of sliding begin to exceed the $\dot{\phi}_{кр}$ (Fig. 2). The equilibrium point appears briefly on the falling section of the adhesion characteristic with a negative slope, which corresponds to negative damping and helps to reduce the average value of $\alpha_э$, and increase in amplitude $\dot{\phi}_{ка}$. Therefore, you can judge the nature of the process of implementing traction by the size of $\alpha_э$.

Quantitative assessment of dependence of $\alpha_э$ and $\dot{\phi}_{ка}$ from the value of M_* will be obtained by solving the nonlinear equation (1) by the numerical quadrature method.

The calculations were performed with the following model parameters:

- $J_к = 1,6 т м^2$; $R_к = 0,625 м$; $\psi_o = 0,32$; $П_o = 250 кН$;
- critical spinning speed $\dot{\phi}_{кр} = 0,1 c^{-1}$;
- relative dynamic vertical load amplitude $\lambda_a = 0,1$;
- oscillation frequency $\lambda(t)$ is taken for f = 10 Hz ($\omega = 62,8 c^{-1}$);
- maximum bite point $M_c^{\max} = 50 кНм$.

Initial traction moment $M_{*(t=0)}$ was taken from the conditions of a stable traction regime, which at $\lambda = 0,1$ makes no more than 90% of the maximum bite point.

Normalizing the equilibrium moment M_* to the maximum bite point $M_c^{\max} = M_c\left(\dot{\phi}_{кр}\right)$ will be set as M∗=ξMcmax.

At the start time, we take $M_{*(t=0)} = 45 кНм$ or $\xi_{(t=0)} = 0,9$.

Then the traction moment increased in proportion to the integration time (at a rate of 1.0 kN m/s) until a breakdown in the boxing mode.

The initial conditions were calculated using the formula $\dot{\phi}_{к(t=0)} = \dot{\phi}_{*(t=0)} = M_{*(t=0)} / \alpha$.

During calculations $\dot{\phi}_к(t)$ we determined the current maximum and minimum values of $\dot{\phi}_к$, by which we calculated the avarages $\dot{\phi}_{кср}$ and amplitude $\dot{\phi}_{ка}$ values of the wheel angular velocity.

$$\dot{\phi}_{кср} = 0,5\left(\dot{\phi}_к^{\max} + \dot{\phi}_к^{\min}\right), \qquad (6)$$

$$\dot{\phi}_{ка} = 0,5\left(\dot{\phi}_к^{\max} - \dot{\phi}_к^{\min}\right), \qquad (7)$$

as well as the value of $\alpha_э$ – by the formula (5).

The calculation results are presented in Fig. 2.

It can be seen from Fig. 2a, b that as the traction moment increases, the amplitude of the angular velocities and wheel pair accelerations increases. It is extremely important to give a quantitative and qualitative assessment of the transition regime, in particular:

- determine the beginning of the transition mode (the beginning of the increase in amplitude);
- determine the boundary conditions for the end of the transition regime and the beginning of spinning.

$\alpha_э$ value gives this assessment.

It is the equivalent damping value that characterizes the process that occurs while wheel contact when creating traction. Such a criterion is invariant with respect to the type of adhesion characteristic. It reflects the result of the interaction of the wheel with the rail.

$\alpha_э = \alpha = const$ is set for traction mode. In this case it's $\alpha = 500\,кНмс$. There is a sharp decrease of $\alpha_э$ at the very beginning of the transition, and with a breakdown of spinning $\alpha_э \approx 0$.

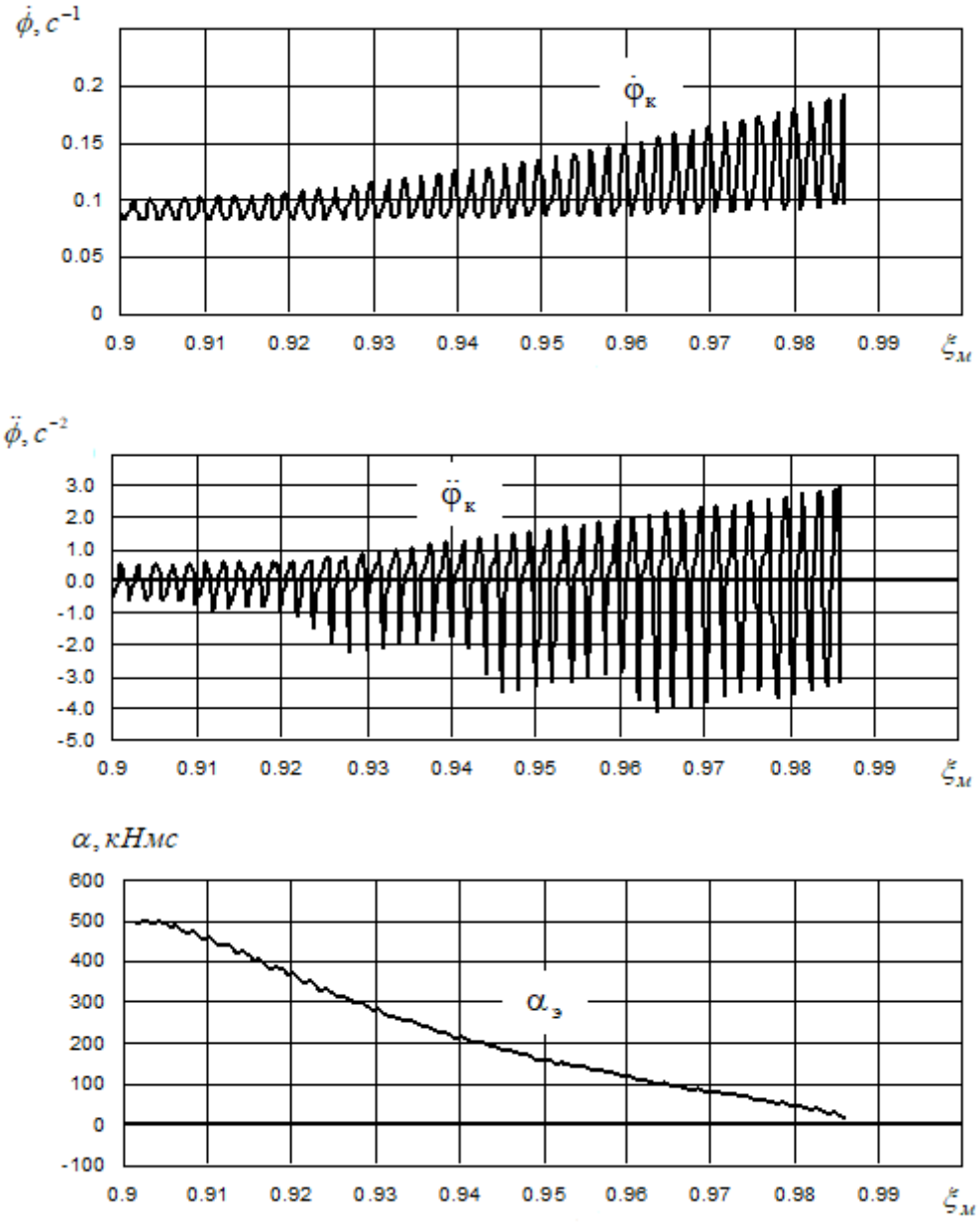

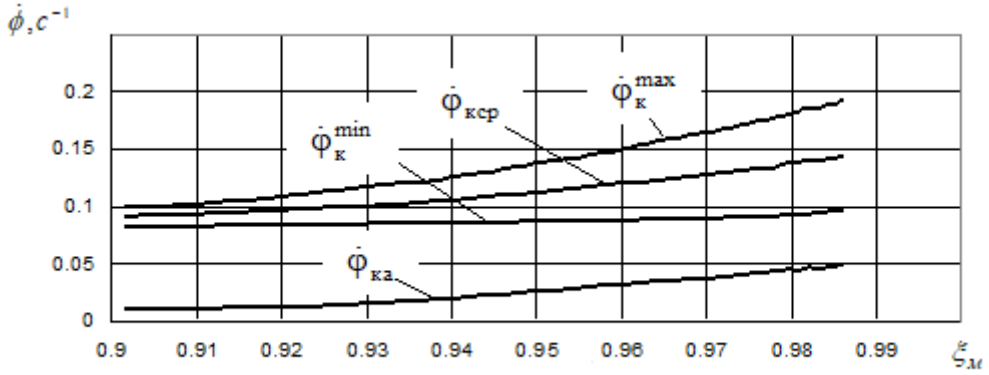

Fig. 2. Dynamic characteristics of the model during transition mode

If you stop the increase of traction moment when the value $\alpha_э$ reaches zero, then we get the maximum stable mode of maximum traction, as even a slight increase in traction moment will lead to a spinning breakdown. Such an extreme steady mode can be considered the final stage of the spinning transition.

Changing $\alpha_э$ affects the dynamic performance of the wheel-motor unit, such as forward axlebox acceleration and the dynamic component of the angular velocity of the wheelset. Let's prove this statement on an extremely simplified mathematical model of a support-frame traction drive - see Fig. 3.

The torsional system in this case consists of a wheel pair and rotating masses of the drive, the inertial torque of which are given to the axis of the wheel pair. There is no kinematic relationship between the angular coordinates of the torsion system and the linear coordinates of the wheelset.

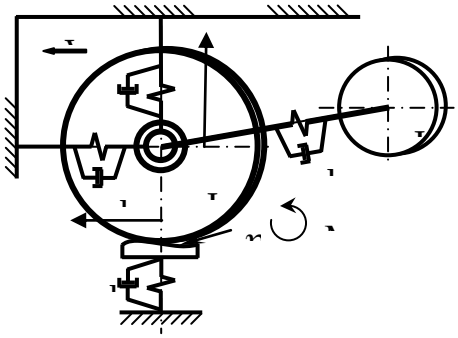

Fig. 3. The design scheme of the traction drive to study the transition from traction to spinning

This model is described by a system of differential equations in dynamic coordinates:

$$\left.\begin{aligned} &J_я\ddot{\phi}_я + b_м\left(\dot{\phi}_я - \dot{\phi}_к\right) + c_м\left(\phi_я - \phi_к\right) = 0;\\ &J_к\ddot{\phi}_к + b_м\left(\dot{\phi}_к - \dot{\phi}_я\right) + c_м\left(\phi_к - \phi_я\right) = -\frac{\Delta П}{П_o}M_* - \alpha\dot{\phi}_{ск};\\ &m_к\ddot{z}_к + \left(b_1 + b_n\right)\dot{z}_к + \left(c_1 + c_n\right)z_к = b_n\dot{\eta} + c_n\eta;\\ &m_к\ddot{x}_к + b_x\dot{x}_к + c_x x_к = \frac{1}{R_к}\left(\frac{\Delta П}{П_o}M_* + \alpha\dot{\phi}_{ск}\right); \end{aligned}\right\}, \quad (8)$$

After substitution of $\dot{\phi}_{ск} = \dot{\phi}_к - \dot{x}_к / R_к$ and $\Delta П = b_n\left(\dot{\eta} - \dot{z}_к\right) + c_n\left(\eta - z_к\right)$ we get:

$$\left.\begin{aligned} &J_я\ddot{\phi}_я + b_м\left(\dot{\phi}_я - \dot{\phi}_к\right) + c_м\left(\phi_я - \phi_к\right) = 0;\\ &J_к\ddot{\phi}_к + b_м\left(\dot{\phi}_к - \dot{\phi}_я\right) + c_м\left(\phi_к - \phi_я\right) + \alpha\left(\dot{\phi}_к - \frac{\dot{x}_к}{R_к}\right) + \frac{M_*}{П_o}\left(b_n\dot{z}_к + c_n z_n\right) =\\ &= -\frac{M_*}{П_o}\left(b_n\dot{\eta} + c_n\eta\right);\\ &m_к\ddot{z}_к + \left(b_1 + b_n\right)\dot{z}_к + \left(c_1 + c_n\right)z_к = b_n\dot{\eta} + c_n\eta;\\ &m_к\ddot{x}_к + b_x\dot{x}_к + c_x x_к + \frac{\alpha}{R_к}\left(\frac{\dot{x}_к}{R_к} - \dot{\phi}_к\right) - \frac{M_*}{R_к П_o}\left(b_n\dot{z}_к + c_n z_n\right) =\\ &= \frac{M_*}{R_к П_o}\left(b_n\dot{\eta} + c_n\eta\right) \end{aligned}\right\} \quad (9)$$

Solving the linear system (9), the spectral densities of the accelerations of the generalized coordinates of the model and their mean square values (RMS) when changing α within 0 – 1000 kNms.

Relative indicators are of practical interest. $\chi(\omega) = \frac{S_x(\omega)}{S_z(\omega)} = \frac{|W_x(\omega)|^2}{|W_z(\omega)|^2}$ and $\chi_{xz}^{\sigma} = \frac{\sigma_{бx}}{\sigma_{бz}}$,

The calculation results are shown in Fig. 4 and Fig. 5. In Fig. 4, the bottom boundaries of the family of curves correspond to the traction mode, and the upper ones correspond to the extreme of the bite mode.

Thus, we take the longitudinal acceleration of the axlebox and the dynamic components of the angular spinning speed of the wheelset as an informative sign of the transition process. An additional informative sign may be their normalized values, if there is information about the vertical accelerations of the axle box.

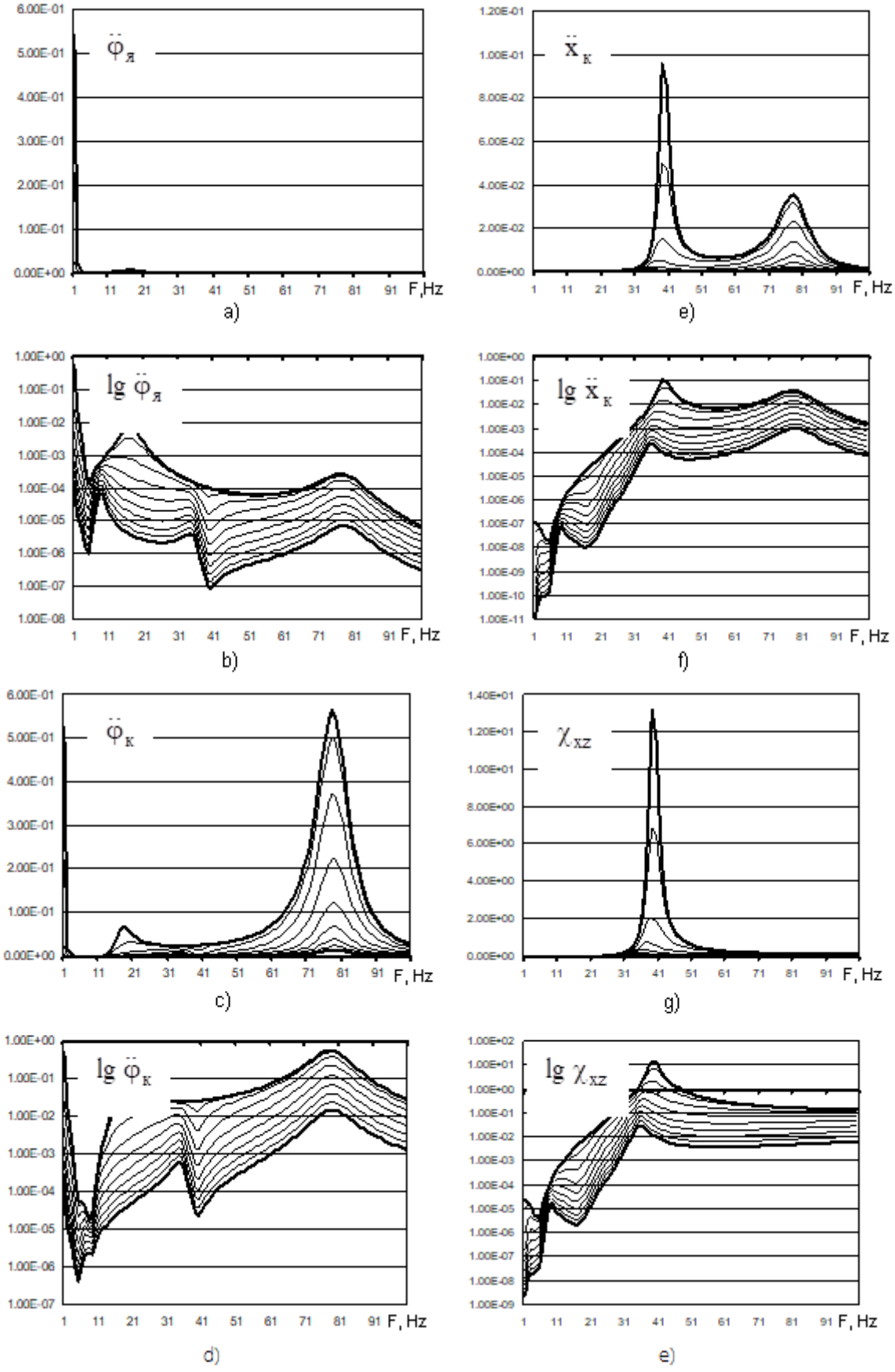

Fig. 4. Spectral acceleration densities of the generalized coordinates of the drive in the transition mode

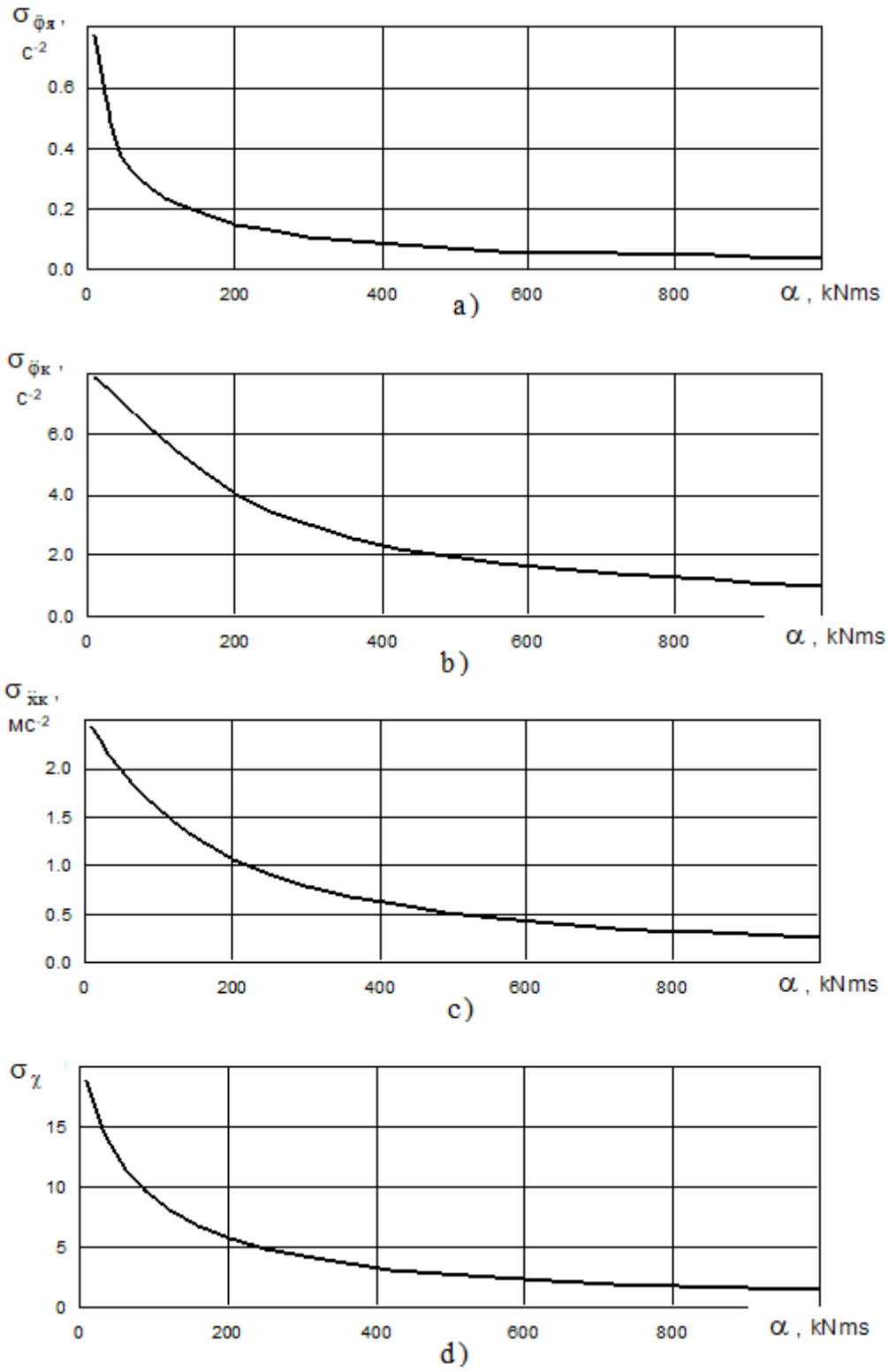

Fig. 5. The rms values of the accelerations of the generalized coordinates and the relative parameter of χ of the support frame drive in transition mode

A characteristic feature of the adopted model of the support-frame drive is that the dynamic processes in it don't depend on the moving direction. In the models there is a difference in the dynamic processes in the drives due to the transport delay of the disturbance under the first and second wheelsets along the way that describe the trolley with two wheel-motor blocks, due to the relationship between the galloping vibrations of the trolley and the vibrations of the torsion drive systems. But this difference is negligible.

As far as we can see in Fig. 5, the amplitudes of the angular accelerations of the wheel pair and the armature significantly change in the transition mode.

This is due to the fact that with a decrease of α the torsion system rushes to non-oscillatory motion with zero frequency, i.e. an increase in the spectral densities of the coordinates of the torsion system in the surrounding frequency $\omega = 0$.

In terms of informativeness, the longitudinal acceleration axleboxes are quite sensitive to changes α : during the transition from traction to spinning, their rms values change by 8 - 10 times. The root-mean-square value of the normalized (to the spectrum of vertical accelerations) spectral density changes by the same amount. Therefore, the need for standardization in the case of a support-frame drive is doubtful. Field tests can answer this question.

The physical meaning of increasing the amplitudes of forward spinning accelerations of the axle box with decreasing equivalent damping in wheel contact is that the dissipative characteristic of the longitudinal connection of the wheel with the rail decreases (almost to zero), and the disturbing effect of the dynamic forces in the wheel contact remains at the same level. This feature of the transition mode is clearly visible in the system analysis (9), in particular, the second and fourth equations. Therefore, the adoption as informative signs of a transitional regime of forward accelerations of axleboxes is quite justified.

In the spinning and use detection device [5], the principle of which is based on the analysis of dynamic processes in the support axial traction drive, acceleration sensors are installed on the traction motor body at the point of its suspension from the carriage frame. But the accelerations at the traction motor attachment point differ from the angular accelerations of the traction motor housing. They contain information about the vibration of the torsion system, as well as about longitudinal and vertical accelerations of the axle box. With a corresponding correction of the signal by installing an additional dual acceleration sensor on the axle box, the efficiency of the recognition of the transition mode increases significantly, which was confirmed experimentally during experimental drive tests.

There are two axle boxes per wheel pair. But it's enough to control the acceleration of one of the axle boxes for the device operation. Additional information about the state of contact of the friction wheel contact to increase the reliability and completeness of the information can be obtained from the sensor of angular velocity (acceleration) of the wheelset.

The parameters measured by the sensors are processed by an electronic computing device according to a certain algorithm [2], as a result of which informative signs of the state of wheel contact are formed. The condition of frictional wheel contact for each wheelset can be conditionally divided, for example, into three specific values:

1. traction mode is stably implemented (the probability of bond failure is almost zero);
2. there are signs of unstable traction (the probability of bond failure is 0.7-0.9);
3. the development of slippage is inevitable at the earliest time (the probability of bond failure is more than 0.9).

Decisions are made in accordance with the condition of friction contact. For condition 1, everything remains unchanged and the traction continues. In condition 2, sand is supplied under the wheels to increase the adhesion forces of the wheel contact. In condition 3, it is urgent to reduce traction to prevent slipping according to a certain law. Maintaining traction at the same level in condition 3 is not advisable, since with the development of spinning, the resulting traction force can fall by 40-60%, and its further restoration will be accompanied by increased wear of the wheels and rails and dynamic loads in the transmission.

Each condition corresponds to a specific digital signal (code), which is fed to the input of the device for controlling traction and sand supply.

III. RESULTS

The installation diagram of the sensors and the main dimensions of the electric locomotive are shown in Fig. 6.

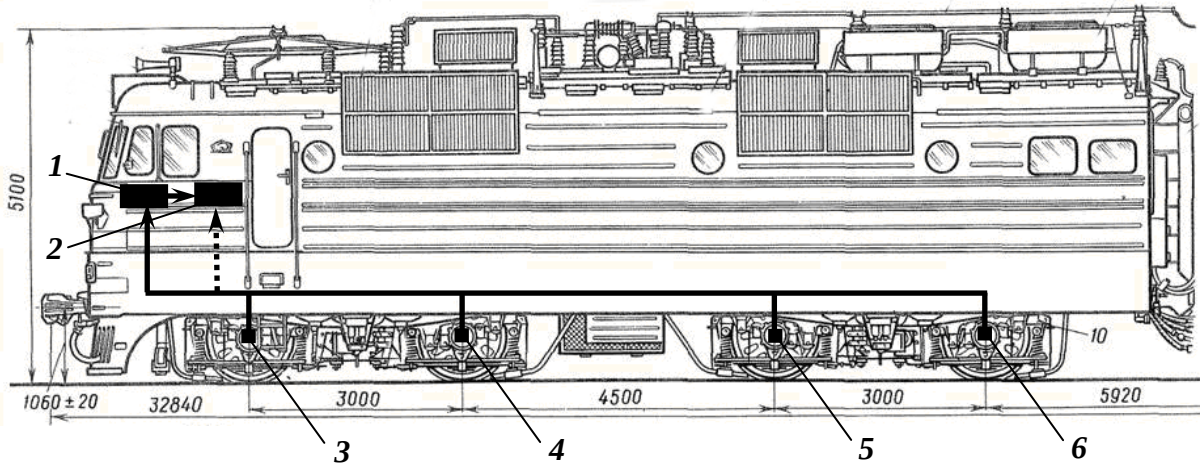

Fig. 6. Installation scheme of sensors on an electric locomotive:
1 - block signal processing sensors; 2 – traction control unit;
3-6 - sensors mounted on axle boxes

In order to maximize noise immunity, the processing of sensor signals must be performed in the immediate vicinity of the sensors themselves, i.e. combine in one structural module both the sensor and the microprocessor, which issues a digital signal to the control device about the condition of the wheel contact with the rails. Then the friction contact state recognition functions (device 1) will be transferred to the microcontrollers located on the axle boxes, and the generated status codes of each wheel pair can be directly transferred to the traction control unit 2 - dashed arrow in Fig. 6.

One of the possible options for placing sensors and a microcontroller on the cover of an electric locomotive axle box is shown in Fig. 7.

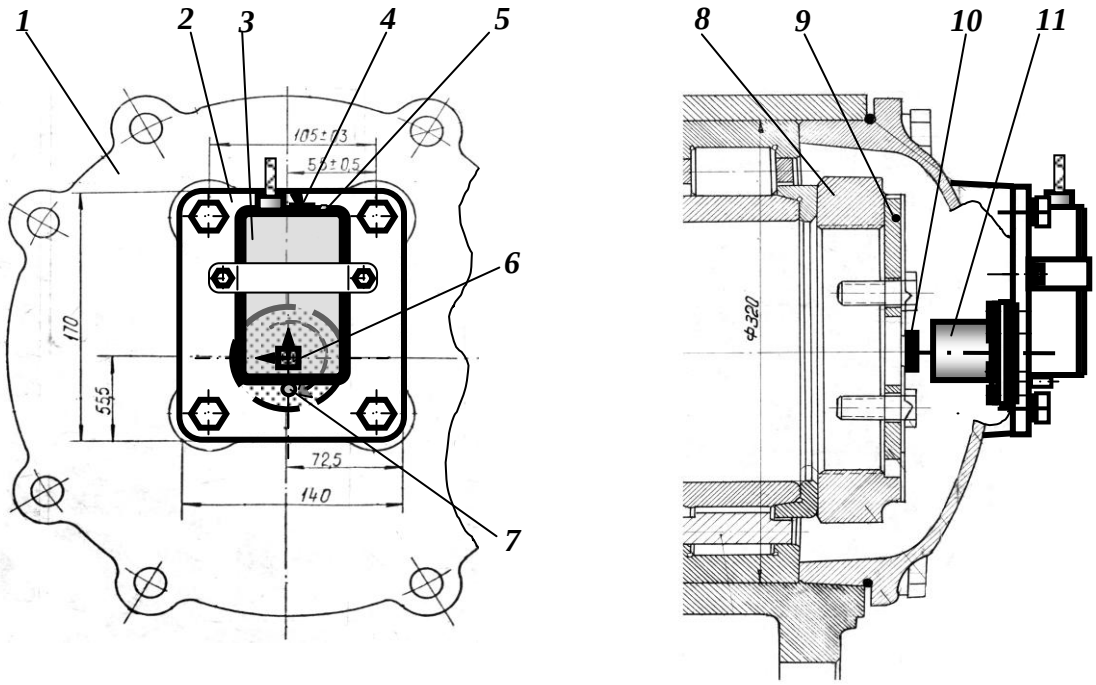

Fig. 7. Installation option of a unit with sensors on the cover of an electric locomotive axle box:
1 - axle box cover; 2 - mounting plate; 3 - electronic unit frame; 4 - block switch;
5 - light indicator of the unit; 6 - three-coordinate accelerometer (inside the frame); 7 - safety pin; 8 - wheel axle nut; 9 - a lock plate of a nut; 10 - permanent magnet;
11 - the housing of the sensor angle of rotation of the wheelset

The presence of microcontrollers in the sensors allows you to implement more complex algorithms for processing information and issuing a signal about the increasing probability of spinning. So, for example, when using a microcontroller with a Cortex-M3 core (examples are STM32F103 [8] and 1986 BE92QI [9]), you can use neural networks trained on an array of data taken from real boxes. This will significantly improve the reliability of slip probability estimation algorithms. The trained neural network, then, can be converted into code for the microcontroller,

And today it is already being implemented in semi-automatic mode (using the X-Cube-AI toolkit [6-9] or its analogs). More complex implementations of neural networks with the possibility of self-learning in the process of work will require an increase in the computing power of the core on board the sensor, but as a result there will be a system that adapts to changes in the wheelset during the entire period of operation.

Thus, the accelerometer sensors and the angle sensor of the axle-wheel pair axis placed on the axle box cover give the axle sensory qualities. And the signal processing microcontrollers located in the immediate vicinity of the sensors turn an ordinary box into a smart box. From the point of view of increasing the intelligence of devices, the sensors of a smart axle box are intelligent sensors.

The main difference between an intelligent sensor and an ordinary is the presence of built-in electronics. However, in different standards the definition of "intelligent", "smart" (according to IEEE terminology [11]) has significant differences. For example, in terms of the Russian standard on intelligent sensors and measuring systems, a mandatory requirement for an intelligent sensor is the presence of additional measures in the sensor using a different physical measurement principle (compared to the basic sensor measure). From the point of view of metrology, the sensor remains a measuring transducer, and by definition it should not contain electronics capable of switching from a converted electrical signal (for example, in volts) to a directly measurable physical quantity (for example, vibration velocity). According to the requirements of metrologists, this is no longer a sensor, but a measuring device (for example, a vibrometer).

The development of technology and the reduction in the cost of electronics, for its part, are shifting the processing and calculating devices closer to the monitoring object. The profit is obvious: instead of transmitting an analog signal subject to noise, it transmits a digital signal (moreover, not a digitized version of the analog signal, but a set of calculated parameters required for the monitoring system). With the development of electronics, it was possible to observe how, at first, blocks with electronics were placed near the sensors at a distance of 30-40 cm, and then the filling of the blocks decreased in size, the blocks were integrated into the cable connectors, and then into the cases of the sensors themselves. The question arises: why do we need such a tight integration of electronics with a sensitive element? Basically, to reduce the cost of cables, it is enough to have an electronic unit integrated with the connector; additional miniaturization is not required to install the electronics in the sensor housing.

Nevertheless, the installation of electronics in the sensor housing gives additional results that are not related to the price of cable management (this stage was completed in 2012-2013). One of the first unexpected results was the possibility of a deep self-diagnosis of the sensor, the presence of electronics inside the sensor made it possible to introduce many of heterogeneous signals directly onto the electronics board without raising the cost of the external connector (as well as without increasing the noise level affecting these service signals). This made it possible to give the sensor the ability to assess the quality of its functioning and working conditions; if a defect was suspected of occurrence and development in the element of the measuring system, a message was popped up indicating that sensor must be replaced.

The second important result was the possibility of full self-calibration and self-monitoring of the sensor. For example, it became possible to generate a reference signal with its transmission to an additional piezo plate for vibration sensors. This allows you to evaluate the operation of the entire measuring path without using a vibration bed.

The introduction of such additional functions in the sensors of physical signals allows you to develop intelligent measuring points that increase not only the registration and transmission of data, but also provide high reliability of the entire measuring system.

Thus, the basis for building a smart axle box is an intelligent sensor that accurately measures the rotation speed of the wheelset (with high resolution in amplitude and a frequency band of at least 100 Hz) and an intelligent sensor that measures vibration acceleration in the frequency band 10 - 2000 Hz with a resolution of low 14-16 bit. Until recently, rotational speed sensors with a resolution of 12 bits or more were not available (or structurally unsuitable for using them in the axle box), however, today, IDM-Plus LLC (Zelenograd) has developed ASIC for constructing high resolution encoders based on rotating magnets [12-18].

Table 1. The main parameters of the encoder chip ENC_ASIC2

Parameter	Value
Supply voltage	5/3,3 ± 10%
Conversion resolution, bit (deg)	12 (0.09)
Conversion time, ns	250
Tracking speed, rpm	> 60,000
Consumption current, mA	30
Maximum frequency of the SPI / SSI interface, not less, MHz	4
Resolution of the built-in temperature sensor, °C	1.5
Rev counter	1–1024
Operating temperature range, °C	–60…+125

The parameters of such a sensor make it possible to use it as the main one for recording the breakdown condition. Moreover, the margin on the sampling frequency (4 MHz) allows the signal to be averaged and thereby increase the resolution of the sensor at lower frequencies. For example, summing 16 consecutive samples of a signal with subsequent decimation of the signal by 16 times allows you to increase the resolution of the conversion to 13 bits (with uncorrelated interference).

National research university of electronic technology MIET (Zelenograd) also developed an ASIC chip for monitoring the state of mechanisms based on vibration data [19-21],

which can be used to create a traction control system that implements the principle of spinning forecasting.

IV. DISCUSSION

The main problem in implementing the assessment of the contact mode of the wheel with the rail is the registration of small fluctuations in the angular velocity of the wheelset. The encoder registers the dependence of the angular coordinate on time (Fig. 8, constant speed movement).

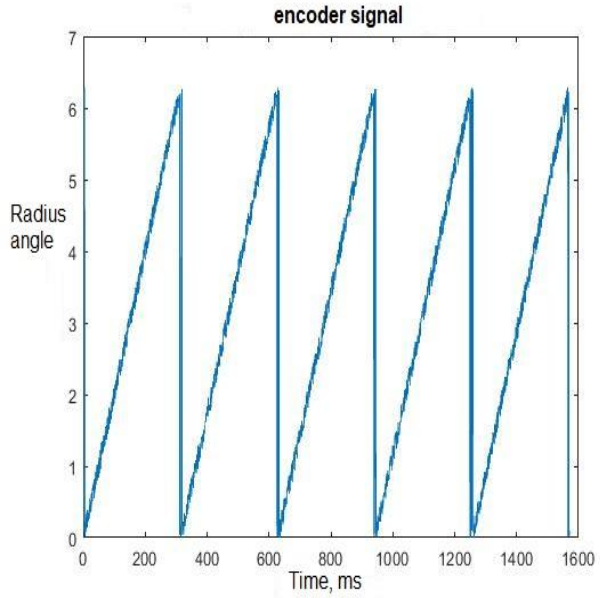

Fig. 8. Encoder signal

The signal is noisy, and is periodic with a period equal to 2*π radians. The frequency can be removed by adding an integer number of revolutions to the corner.

Classical numerical differentiation of this signal by the formula

$$y_i' = \frac{y_{i+1} - y_i}{h}, \qquad (10)$$

leads to significant oscillations in the angular velocity (Fig. 9).

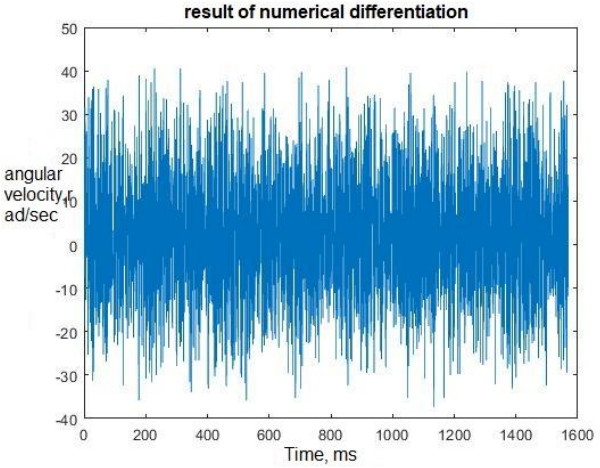

Fig. 9. A numerical estimate of the angular velocity of a pair of wheels based on expression (10)

We use a third-order smoothing cubic spline to evaluate the derivative of a noisy signal [19]

$$p_i(x) = C_{i,1}(x - x_i)^3 + C_{i,2}(x - x_i)^2 + C_{i,3}(x - x_i) + C_{i,4}, (11)$$

The smoothing spline differs from the interpolation one in that the requirement of the spline graph passing through the given points is replaced by a compromise between the two following requirements:

- the spline chart should lie as close to the given points as possible;
- the smoothness of the resulting curve should be as large as possible.

Let f (x) be the smoothing spline, and $(x_k, y_k)_{k=1,2,...,n}$ be the input data. As a measure of the smoothness of the spline f (x), we choose the integral characteristic of its derivative

$$F(f) = \int_{x_1}^{x_n} \left(\frac{d^m f}{dx^m} \right)^2 dx, \qquad (12)$$

where m is a number, that $2m$ is the order of the spline, which for a cubic spline is 4 (degree minus 1), i.e. for a cubic spline, the measure of smoothness is

$$F(f) = \int_{x_1}^{x_n} \left(\frac{d^2 f}{dx^2} \right)^2 dx, \qquad (13)$$

As a measure of proximity choose a weighted total deviation of the spline from the source data:

$$E(f) = \sum_{k=1}^{n} w_k (y_k - f(x_k))^2, \qquad (14)$$

At this point the weight w_k are usually chosen as the weights of the generalized quadrature formula of the trapezoid. Then we can set some accuracy ε and look for a smoothing spline that minimizes the expression

$$\rho \cdot E(f) + F(f), \qquad (15)$$

where the parameter ρ is chosen from the condition $E(f) \le \varepsilon$.

To find the coefficients Cik of the spline (11) taking into account the minimization of expression (15), it is necessary to solve a system of N linear equations with a 5-diagonal matrix with a positive main diagonal. Such systems are quite well solved by the sweep method [19, 22-26]. The approximation by the smoothing spline allows, in addition to the function itself (in our case, this is the angle), to obtain its two continuous derivatives (angular velocity and acceleration) (Fig. 10).

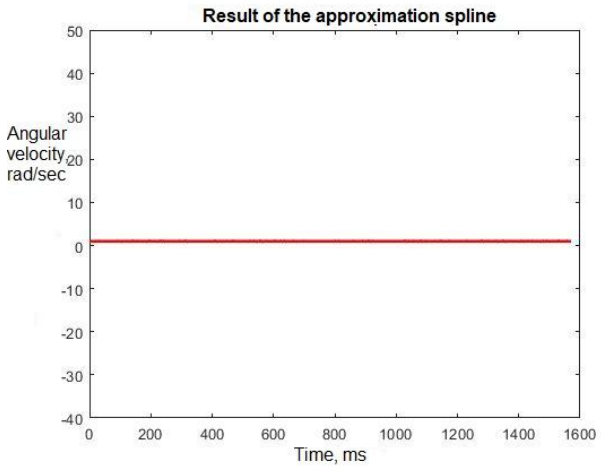

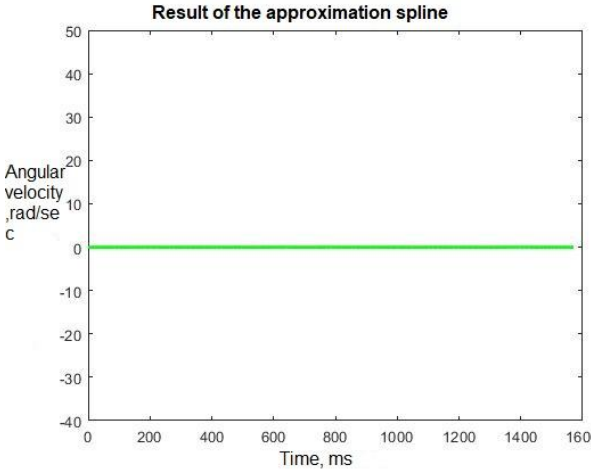

Fig. 10. The result of estimating angular velocity and angular acceleration using a smoothing spline

The result on a larger scale (Fig. 11):

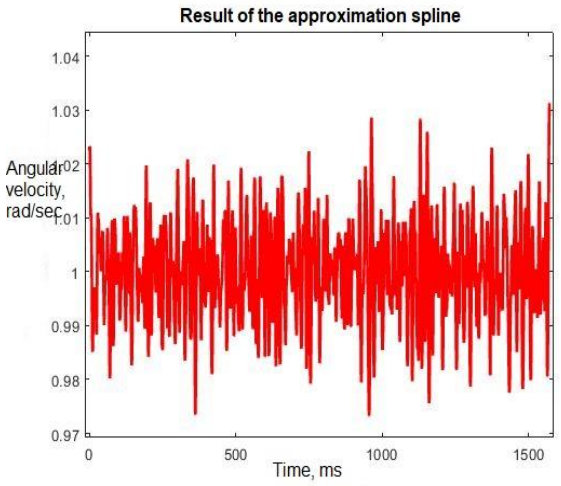

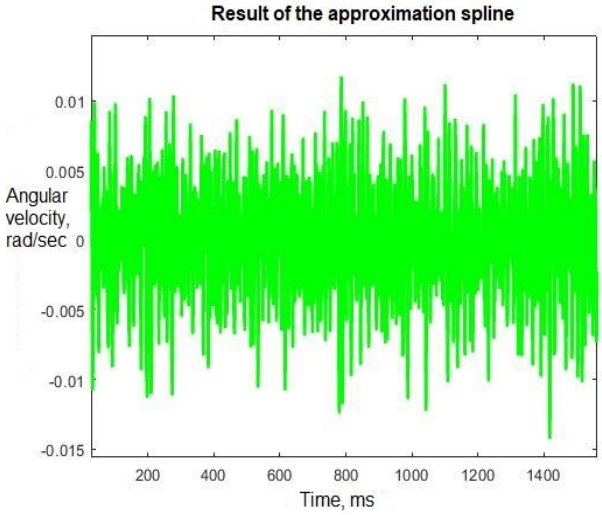

Fig. 11. The result of evaluating angular velocity and angular acceleration on a large scale.

As one can see from the figure, the oscillations in comparison with the classical digital differentiation decreased by 3,000 times! The angular speed of 1 rad/sec corresponds to the movement mode with a constant linear speed of 71 km/h. The angular acceleration in this case is 0. A further decrease in the oscillations can be carried out in two ways:

- preliminary median filtering with a window equal to 25 ms (for a band of 100 Hz);
- an increase in the smoothing parameter ρ for the spline approximation to values close to 1 [27-29].

V. CONCLUSION

Equipping the axle box with sensors combined with information processing microchips transpasses it into a series of smart devices that can collect and analyze information up to the level of signal output for decision-making.

The basis of the smart box decision block can be a neural network, the inputs of which are fed from the scores of an encoder, a vibroaccelerometer of longitudinal and transverse accelerations, as well as a temperature sensor. The output of the neural network is a signal characterizing the state of the box (basic, transient mode, failure mode).

The first neural network (Fig. 12) is used to assess the condition of the axle box bearing according to the RMS/Peak ratio for high-frequency vibration data, RMS vibration acceleration or low-frequency vibration velocity, and also based on the analysis of harmonics of the envelope spectrum of narrow-band high-frequency vibration. This neural network provides signs of bearing degradation, as well as signals of a preemergence or emergence condition of the bearing.

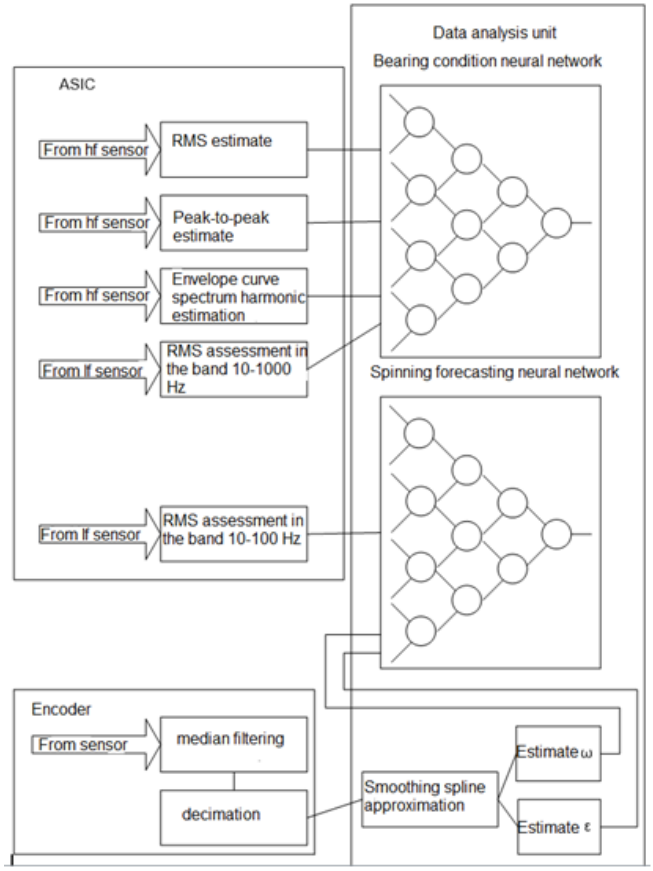

Fig. 12. The structure of digital data processing in a smart box

The second neural network predicts a possible beginning of the process of disruption of traction and transition to the user mode. All digital processing is distributed between the ASIC of the vibration sensor, the ASIC of the encoder and the microcontroller of the processing and data analysis unit. As you can see from Fig. 21 processing is well parallelized, at each stage the amount of data is reduced by several orders of magnitude. So, if analog data is digitized at a frequency of 250,000 Hz, then the data frequency from the ASIC vibrations arrives at a frequency of 10 Hz at the input of a neural network, and at a frequency of 500 Hz from the encoder. Neural networks generate data with a frequency of 5-10 Hz (this is sufficient for making management decisions).

Intelligent sensors of such a system can be placed directly on the lid of the axle box, which will require minor refinement of the design of the lid only, and minimal changes to the traction control system with axial power control. Such smart axle boxes can be used not only on the newly created traction rolling stock, but also for the modernization of the existing railway. We emphasize that the system for early recognition of coupling-limit modes can also be used during braking to exclude spinning.

Using such systems is extremely important for urban rail transport, which in its dynamic qualities should not be inferior to road transport.

ACKNOWLEDGMENT

This work was supported by the Ministry of Education and Science of the Russian Federation under the Agreement on the provision of subsidies No. 14.581.21.0030 dated October 23, 2017, a uniqueness identifier of the project RFMEFI58117X0030.

REFERENCES

1. V.V. Kochergin, "Experimental study of traction drives of locomotives", *Bulletin of VNIIZHT, 8:* 7-10, 1977.
2. P. A. Koropets, V. S. Cherny, *Pat. 2175612 RF, MKI B 60 L 3/10. A device for detecting traction limits of a traction drive of a rail transport.* No. 2000100712/28; declared 01/10/2000; publ. 11/10/2001, Bull. Number 31.
3. P. A. Koropets, *Development and testing of a prototype of the control system for the adhesion of the wheels of a locomotive with rails. Report on research*. Rostov-on-Don, 2009. No. GR 02200952897
4. P. Koropets, *Monitoring wheel-rail contact in traction and braking modes*. LAP LAMBERT Academic Publisher, 2012.
5. A. A. Pavlenko, A. P. Pavlenko, V. B. Klepnikov et al. *Pat. 2071197 RF, MKI6 V 60 L 3/10. A device for detecting boxing and skidding of wheels of a rail vehicle.* No. 94044536/11; declared 12/14/94; publ. 12/27/96, Bull. Number 36.
6. M. V.Nutskova, M. V.Dvoynikov, V. N. Kuchin, "Improving the quality of well completion in order to limit water inflows", *Journal of Engineering and Applied Sciences, 12* (22): 5985-5989, 2017.
7. A. A.Melekhin, S. E.Chernyshov, P. A. Blinov, M. V. Nutskova, "Study of lubricant additives to the drilling fluid for reducing the friction coefficient during well construction with rotary steerable system", *Neftyanoe Khozyaystvo - Oil Industry, 10*: 52-55, 2016.
8. "STM32F103RE Mainstream performance line ARM Cortex-M3 MCU". Retrieved from https://www.st.com/content/st_com/en/products/microcontrollers-microprocessors/stm32-32-bit-arm-cortex-mcus/stm32 -mainstream-mcus / stm32f1-series / stm32f103 / stm32f103re.html (accessed: 04.12.2019).
9. "K1986BE92QI - specifications, documentation". Retrieved from https://ic.milandr.ru/products/mikrokontrollery_i_protsessory/32_razryadnye_mikrokontrollery/1986ve9kh_yadro_arm_cortex_m3/k1986ve92qi/ (accessed: 12.12.2019).
10. "X-CUBE-AI - AI Expansion Pack for STM32CubeMX". Retrieved from https://www.st.com/en/embedded-software/x-cube-ai.html (accessed: 08.12.2019).
11. "IEEE P1451.1 Standard for Smart Transducer Interface, Transducer Electronic Data Sheet and Transducer Interface Specification, Draft 1.40," IEEE Standards Association, 11-16-95.
12. M. V. Nutskova, K. S. Kupavyh, "Improving the quality of well completion in deposits with abnormally low formation pressure", *International Journal of Applied Engineering Research, 11* (11): 7298-7300, 2016.
13. K. S. Kupavikh, M. V. Nutskova, "Ecological features of oil well repair at low-permeability reservoir", *International Journal of Applied Engineering Research, 11* (11): 7505-7508, 2016.
14. G. V. Prokofiev, V. G. Stakhin, V. V. Misevich, B. L. Krivtz, M. A. Kosolapov, "Development of a Magnetic Precision Position Sensor Based on Multipolar Magnetic Technology", *International Journal of Applied Engineering Research, 13* (23): 16656-16661, 2018. ISSN 0973-4562.
15. G. V. Prokofiev, V. G. Stakhin, M. A. Kosolapov, "Development of a specialized microcircuit for a magnetic precision position sensor based on multipolar magnetic technology", *International Journal of Applied Engineering Research, 14* (22): 4143-4148, 2019.
16. G. V. Prokofiev, K. N. Bolshakov, V. G. Stakhin, "Development of ASIC for Sine-Cosine to Position Code Conversion with High Resolution", *International Journal of Applied Engineering Research, 11* (21): 10441-10446, 2016. ISSN 0973-4562.
17. G. Prokofiev, K. Bolshakov, V. Stakhin, "Integrated position processor for precision motion control systems for moving units and mechanisms", Components and technologies, 7: 81-86, 2016.
18. G. Prokofiev, B. Stakhin, R. Germanov, "Small-sized angular position sensors based on a single-chip magnetic encoder microcircuit. SO-TIME ELECTRONICS No. 8 2016 C.2-6.
19. V. V. Nosach, *Solving approximation problems using personal computers.* Moscow: MIKAP, 1994.
20. S. Lebedev, S. Sinyutin, D. Skvortsov, A. Grigoryev, "Intelligent bearing control unit for control systems for motor drives, rotating units and mechanisms*", Modern Electronics, 8:* 60-62, 2018.

21. D. G. Lukin, D. A. Yungmeister, A. I. Yacheikin, A. I. Isaev, "Improvement of shield machine KT1-5.6M cutterhead operation", *Gornyi Zhurnal, 12:* 73-77, 2018.
22. I. Bashir, B. Zaghari, T. J. Harvey, A. S. Weddell, N. M. White, L. Wang, "Design and Testing of a Sensing System for AeroEngine Smart Bearings", *MDPI Proceedings, 2* (1005), 2018. DOI: 10.3390/proceedings2131005
23. D. A. Yungmeister, S. E. Ivanov, A. I. Isaev, "Calculation of parameters of technological equipment for deep-sea mining", *IOP Conference Series: Materials Science and Engineering, 327* (2), 022050, 2018.
24. A. Trilla, P. Gratacòs, "Maintenance of bogie components through vibration inspection with intelligent wireless sensors: A case study on axle-boxes and wheel-sets using the empirical mode decomposition technique", *Proceedings of the Institution of Mechanical Engineers, Part F: Journal of Rail and Rapid Transit, 230* (5): 1408-1414, 2016. DOI: 10.1177/0954409714560798
25. I. Bashir, L.-J. Wang, T. Harvey, B. Zaghari, A. S. Weddell, N. M. White. "Integrated smart bearings for next generation aero-engines Part 1: Development of a sensor suite for automatic bearing health monitoring.", *WCCM2017, 12,* 2017.
26. R. Yu. Urazbakhtin, D. A. Yungmeyster, "The results of studies of the tunneling rescue complex for coal mines*", IOP Conference Series: Materials Science and Engineering, 560* (1), 012130, 2019.
27. O. Ponomarenko, "Adjustment of the technology of the containment of freight wagons when extending the period of their operation", *Transportation systems and technologies, 1* (32): 147-153, 2018.
28. P. Shi, X. Liu, M. Liu, "Scattering of harmonic antiplane shear waves by an arc-shaped interfacial crack in functionally graded annular bi-material guide rail", *Mechanics Based Design of Structures and Machines,* 2019. DOI: 10.1080/15397734.2019.1657891
29. F. Marques, H. Magalhães, B. Liu, J. Pombo, P. Flores, J. Ambrósio, J. Piotrowski, S. Brunni, "On the generation of enhanced lookup tables for wheel-rail contact models", *Wear, 434-435,* 202993, 2019. DOI: 10.1016/j.wear.2019.202993